

Non-Invasive Absolute Temperature Imaging with TmDOTMA⁻

J. R. James¹, S. K. Hekmatyar², Y. Gao², M. A. Miller², P. Hopewell², A. Babsky², and N. Bansal²

¹School of Health Sciences, Purdue University, West Lafayette, Indiana, United States, ²Department of Radiology, Indiana University School of Medicine, Indianapolis, Indiana, United States

Introduction:

We have devised a novel method for imaging absolute temperature *in vivo* using the strong chemical shift dependence of TmDOTMA⁻ on temperature ($C_T = 0.57\text{ppm}/^\circ\text{C}$)^{1,2} and water signal as a reference. Absolute temperature measurements from phase-sensitive images of TmDOTMA⁻ and water obtained via gradient echo (GE) and asymmetric spin echo (SE) imaging sequences were validated and demonstrated using a TmDOTMA⁻ gel phantom. The feasibility of imaging absolute temperature in rats is demonstrated.

Methods:

TmDOTMA⁻ was synthesized from TmCl₃ (Aldrich, USA) and Na₄DOTMA (Macrocyclics, USA). MR experiments on phantoms were performed using 2 mM TmDOTMA⁻ prepared in 4% agrose on a Varian, 9.4 T, 89 mm vertical bore MR scanner. Three fiber-optic probes (FOPs) were placed in the gel at different locations for calibration and validation purposes. 3D water and TmDOTMA⁻ images were acquired using GE (TR = 500 ms and 23.2 ms for water and TmDOTMA⁻ resp., TE = 0.856 ms, data matrix = 64x64x8, FOV = 3x3x5 cm) and SE (TR = 500 ms and 23.2 ms for water and TmDOTMA⁻ resp., TE = 1.9 ms, phdelay (τ) = 225 μs , data matrix = 64x64x8, FOV = 3x3x5 cm) sequences. CHESS technique was used to suppress unwanted water signal in TmDOTMA⁻ images. Pixel-by-pixel maps of frequency difference between TmDOTMA⁻ and water signal were calculated using the following relation:

$$F = (tof_{TmDOTMA} - tof_{H_2O}) - \left[\frac{\Delta\Phi}{360 \times \text{refrq} \times \tau} \right] + \frac{\text{wrap}}{\text{refrq} \times \tau} \quad [F: \text{Frequency maps from TmDOTMA}^- \text{ and water images; } tof: \text{Transmitter frequency (Hz); } \Delta\Phi: \text{Phase difference between TmDOTMA}^- \text{ and water image; } \text{refrq}: \text{Reference frequency} = 400.396 \text{ Hz; } \tau: \text{Echo time} = 856 \mu\text{s (GE); } \text{phDelay} = 225 \mu\text{s (SE); } \text{wrap} = 1, 2, 3 \dots n \text{ which is incremented during each phase wrap}]$$

The average frequency of 6x6x3 pixels around each FOP was calibrated against the corresponding FOP temperatures. The phantom experiments were repeated twice and the calibration constants from the first set of experiments were used to compute the absolute temperature images. The accuracy and precision of temperature imaging was evaluated by comparing image and fiber-optic temperatures. The effects of B₀ inhomogeneity on absolute temperature imaging was evaluated by comparing temperature images acquired before and after misadjusting the currents in X, Y, XY and X²Y² shim coils. Processing of images was performed on Matlab.

In vivo temperature imaging of Fisher rats (70-110 g) was performed on a Varian 9.4 T, 31cm horizontal bore MR scanner using a 63 mm diameter birdcage coil. Rats were infused with 1 to 1.5 ml of 100 mM TmDOTMA⁻ through the jugular vein. 3D coronal images of water and TmDOTMA⁻ were acquired using GE sequence (TR = 500 ms and 16ms for water and TmDOTMA⁻ resp., TE = 0.92 ms, data matrix = 64x64x8 zero-filled to 256x128x16, FOV = 12x6x5 cm), A 2D multi-slice GE high resolution water image (TR = 20 ms, TE = 2.9 ms, data matrix = 512x128x32, FOV = 12x6 cm) was obtained for anatomical comparison.

Results and Discussion:

Calibration results yielded a slope and intercept of $0.632 \pm 0.001 \text{ ppm}/^\circ\text{C}$ and $-124.59 \pm 0.04 \text{ ppm}$ for GE sequence and $0.646 \pm 0.003 \text{ ppm}/^\circ\text{C}$ and $-125.09 \pm 0.10 \text{ ppm}$ for SE sequence, respectively. Regression analysis between temperatures from FOP and TmDOTMA⁻ images obtained from GE and SE had a slope of 0.99 and 0.969, intercept of 0.614 and 0.760 and an R² of 0.99 for both, respectively. The average difference between the temperatures from FOP and TmDOTMA⁻ images were -0.548°C (GE) and 0.434°C (SE). The accuracy of imaging absolute temperature with TmDOTMA⁻ is computed to be 0.1-0.3°C considering an accuracy of 0.3°C for FOP as per manufacturer specifications.

Absolute temperature measurement from TmDOTMA⁻ was found to be insensitive to the magnetic field inhomogeneities. The average absolute temperature from TmDOTMA⁻ MR images acquired before and after misadjusting the shim currents were $17.02 \pm 0.19^\circ\text{C}$ and $17.10 \pm 0.14^\circ\text{C}$, respectively. The temperature measurements are insensitive to B₀ inhomogeneities because they produce an identical shift in water and TmDOTMA⁻ frequencies.

The feasibility of imaging absolute temperature with TmDOTMA⁻ in a rat *in vivo* is shown in Fig 2. After injecting $\sim 1.4 \text{ mmol/kg}$ TmDOTMA⁻, 3D TmDOTMA⁻ images were acquired (imaging time = $\sim 3 \text{ min}$). The images have $1.88 \times 1.88 \text{ mm}^2$ in-plane resolution, a 7 mm slice thickness and an SNR of 6. The average animal temperature was observed to be 35.92°C when the rectal temperature was 36.75°C . Absolute temperature map from a representative coronal slice shows the heterogeneous temperature distribution in the body with a minimum of 32.56°C caudally and a progressive increase of up to a 40.19°C in the interscapular region which comprises of brown adipose tissue (Fig 2c). This region is known to generate more heat than other parts of the body³. The heart was observed to be at 38.33°C while the abdomen was at 36°C . The fused high-resolution water and temperature image shows the correspondence of the aforementioned temperatures with its respective anatomical features (Fig 2d). The fusion of images was performed on IVA (INDYPET image visualization software).

Conclusions:

Phase-sensitive imaging of TmDOTMA⁻ using water as a reference has proved to be a promising tool for imaging absolute temperature with an 0.1-0.3°C accuracy, $\sim 3 \text{ min}$ temporal resolution and $\sim 2 \text{ mm}$ spatial resolution. The developed method shows excellent correlation with the temperature measured by FOP and is insensitive to magnetic field inhomogeneities. Imaging absolute temperature with TmDOTMA⁻ should prove useful in numerous biomedical applications, such as the diagnosis of certain pathological conditions on the basis of temperature in deep-seated organs as well as monitoring of temperature during hypothermia and hyperthermia treatment.

References: (1) Hekmatyar SK, et. al., *Magn. Reson. Med.*, 53: 294-303, 2005. (2) Pakin SK, et. al., *NMR in Biomedicine*, 18:1-9, 2005. (3) Closa D, et. al., *Exper. Phys.*, 78: 243-253, 1993.

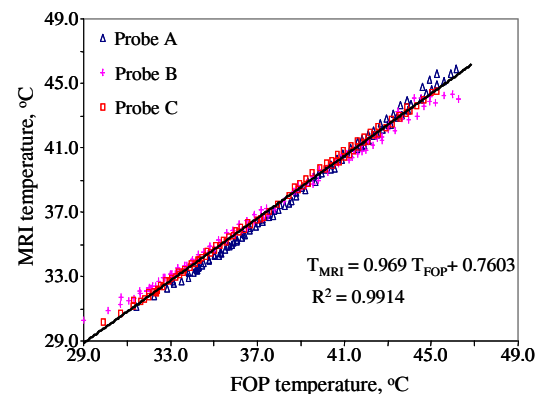


Fig 1: Plot showing correlation between regional temperatures from the FOP and absolute temperatures computed from the phase shift of TmDOTMA⁻ in 6x6x3 pixels around each FOP for SE imaging sequence.

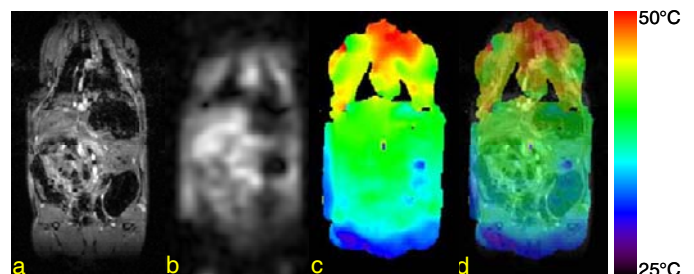


Fig 2: Representative coronal slice of *in vivo* (a) high resolution ¹H image, (b) methyl signal from TmDOTMA⁻, (c) temperature map and (d) temperature map fused with high resolution water image showing heterogeneous temperature distribution.